

## Hydrogen Atom Transfer (HAT) Processes Promoted by the Quinolinimide-N-Oxyl Radical. A Kinetic and Theoretical Study

Gino A. DiLabio, Paola Franchi, Osvaldo Lanzalunga, Andrea Lapi, Fiorella Lucarini, Marco Lucarini, Marco Mazzonna, Viki Kumar Prasad, and Barbara Ticconi

*J. Org. Chem.*, **Just Accepted Manuscript** • Publication Date (Web): 23 May 2017

Downloaded from <http://pubs.acs.org> on May 24, 2017

### Just Accepted

“Just Accepted” manuscripts have been peer-reviewed and accepted for publication. They are posted online prior to technical editing, formatting for publication and author proofing. The American Chemical Society provides “Just Accepted” as a free service to the research community to expedite the dissemination of scientific material as soon as possible after acceptance. “Just Accepted” manuscripts appear in full in PDF format accompanied by an HTML abstract. “Just Accepted” manuscripts have been fully peer reviewed, but should not be considered the official version of record. They are accessible to all readers and citable by the Digital Object Identifier (DOI®). “Just Accepted” is an optional service offered to authors. Therefore, the “Just Accepted” Web site may not include all articles that will be published in the journal. After a manuscript is technically edited and formatted, it will be removed from the “Just Accepted” Web site and published as an ASAP article. Note that technical editing may introduce minor changes to the manuscript text and/or graphics which could affect content, and all legal disclaimers and ethical guidelines that apply to the journal pertain. ACS cannot be held responsible for errors or consequences arising from the use of information contained in these “Just Accepted” manuscripts.



1  
2  
3  
4  
5  
6  
7  
8  
9  
10  
11  
12  
13  
14  
15  
16  
17  
18  
19  
20  
21  
22  
23  
24  
25  
26  
27  
28  
29  
30  
31  
32  
33  
34  
35  
36  
37  
38  
39  
40  
41  
42  
43  
44  
45  
46  
47  
48  
49  
50  
51  
52  
53  
54  
55  
56  
57  
58  
59  
60

# Hydrogen Atom Transfer (HAT) Processes

## Promoted by the Quinolinimide-*N*-Oxyl Radical.

### A Kinetic and Theoretical Study

Gino A. DiLabio,<sup>a</sup> Paola Franchi,<sup>c</sup> Osvaldo Lanzalunga,<sup>b\*</sup> Andrea Lapi,<sup>b</sup> Fiorella Lucarini,<sup>d</sup> Marco  
Lucarini,<sup>c</sup> Marco Mazzonna,<sup>b</sup> Viki Kumar Prasad,<sup>a</sup> and Barbara Ticconi<sup>b</sup>

<sup>a</sup> Department of Chemistry, University of British Columbia, Okanagan, 3247 University Way,  
Kelowna, British Columbia, Canada V1V 1V7

<sup>b</sup> Dipartimento di Chimica, Sapienza Università di Roma and Istituto CNR di Metodologie  
Chimiche (IMC-CNR), Sezione Meccanismi di Reazione, c/o Dipartimento di Chimica, Sapienza  
Università di Roma, P.le A. Moro, 5 I-00185 Rome, Italy

<sup>c</sup> Dipartimento di Chimica “G. Ciamician”, Università di Bologna, Via San Giacomo 11, I-40126  
Bologna, Italy

<sup>d</sup> Département de Chimie, Université de Fribourg, Chemin du Musée 9, 1700 Fribourg, Switzerland

Email: [osvaldo.lanzalunga@uniroma1.it](mailto:osvaldo.lanzalunga@uniroma1.it)

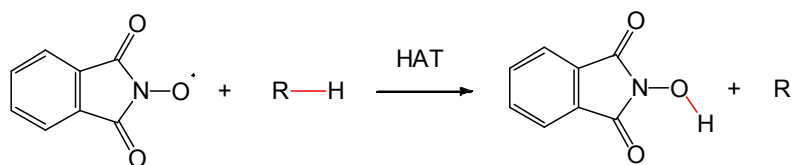
ABSTRACT: A kinetic study of the hydrogen atom transfer (HAT) reactions from a series of  
organic compounds to the quinolinimide-*N*-oxyl radical (QINO) was carried out in CH<sub>3</sub>CN. The  
HAT rate constants are significantly higher than those observed with the phthalimide-*N*-oxyl radical  
(PINO) as a result of enthalpic and polar effects due to the presence of the *N*-heteroaromatic ring in

1  
2  
3 QINO. The relevance of polar effects is supported by theoretical calculations carried out for the  
4  
5 reactions of the two *N*-oxyl radicals with toluene which indicate that the HAT process is  
6  
7 characterized by a significant degree of charge transfer enabled by the  $\pi$ -stacking that occurs  
8  
9 between the toluene and the *N*-oxyl aromatic rings in the transition state structures. An increase of  
10  
11 the HAT reactivity of QINO was observed in the presence of  $\text{HClO}_4$  0.15 M and  $\text{Mg}(\text{ClO}_4)_2$  0.15 M  
12  
13 due to the protonation or complexation with the Lewis acid of the pyridine nitrogen that leads to a  
14  
15 further decrease of the electron density in the *N*-oxyl radical. These results fully support the use of  
16  
17 *N*-hydroxyquinolinimide (NHQI) as a convenient substitute of *N*-hydroxyphthalimide (NHPI) in the  
18  
19 catalytic aerobic oxidations of aliphatic hydrocarbons characterized by relatively high C-H bond  
20  
21 dissociation energies.  
22  
23  
24  
25  
26  
27

## 28 Introduction

29  
30 The use of *N*-hydroxyphthalimide (NHPI) as catalyst in the aerobic oxidative functionalization  
31  
32 of hydrocarbon has attracted a great attention in recent years. In the presence of metal and nonmetal  
33  
34 co-catalysts, the NHPI/ $\text{O}_2$  system was found to efficiently catalyze the introduction of oxygenated  
35  
36 groups in aliphatic and alkylaromatic hydrocarbons.<sup>1</sup>  
37

38 The key role played in the catalytic cycle by the hydrogen atom transfer from the organic substrate  
39  
40 to the phthalimide-*N*-oxyl radical (PINO) (HAT process, Scheme 1) has stimulated several kinetic  
41  
42 studies aimed at obtaining quantitative information on the reactivity of PINO and other structurally  
43  
44 related short-lived *N*-oxyl radicals towards a variety of C-H bonds.<sup>2,3</sup>  
45  
46  
47  
48  
49



56  
57  
58  
59  
60  
**Scheme 1**

The HAT reactivity of short-lived *N*-oxyl radicals is strongly dependent on enthalpic effects based on the difference between the O-H bond dissociation energy (BDE) in the *N*-hydroxy derivative and the C-H BDE of the substrates (eq 1). In this respect the high reactivity of PINO is associated with relatively high NO-H BDE in NHPI (87 kcal/mol).<sup>4</sup>

In addition to enthalpic effects, polar effects also play an important role in the HAT reactivity of *N*-oxyl radicals.<sup>6</sup> The HAT transition state (TS) structure is characterized by a partial degree of charge transfer from the substrate to the *N*-oxyl radical (Figure 1). The polar contribution is clearly dependent on the ability of the substrate and the *N*-oxyl radical to stabilize, respectively, the positive and negative charges developing in the transition state (TS).

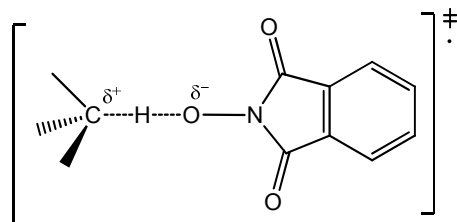


**Figure 1.** Polar transition state in the HAT process promoted by PINO

On the basis of enthalpic considerations, an increase in the HAT reactivity of *N*-oxyl radicals can be established by an increase of  $BDE_{NO-H}$  values of the corresponding *N*-hydroxy derivatives. In aryl substituted *N*-hydroxyphthalimides and other aromatic hydroxylamines an increase of  $BDE_{NO-H}$  values is observed with electron withdrawing aryl substituents which destabilize the resonance structure with charge separation shown in Figure 2.<sup>7</sup>

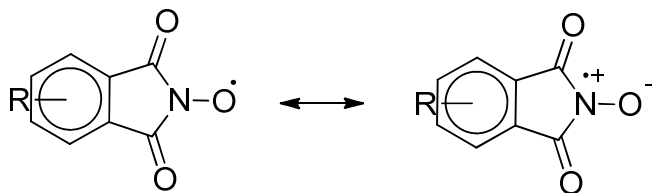
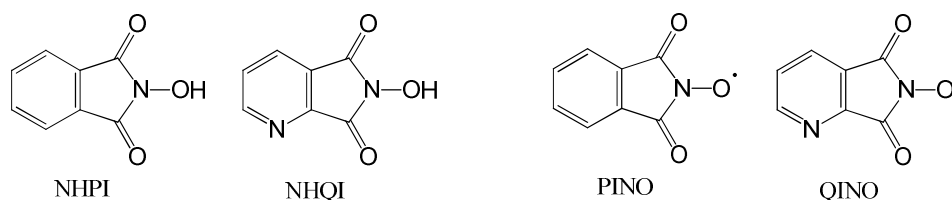


**Figure 2.** Resonance structures of aryl substituted PINO radicals

1  
2  
3  
4  
5 Electron withdrawing substituents are also able to increase the reactivity of the *N*-oxyl radical  
6 through polar effects on the HAT TS structure as a result of enhanced stabilization of the partial  
7 negative charge that develops on the *N*-oxyl radical at the TS.<sup>8</sup> The enhancement of HAT reactivity  
8 exerted by electron withdrawing substituents on *N*-oxyl radicals has been reported in several kinetic  
9 and product studies of the reaction of aryl substituted PINO and benzotriazole-*N*-oxyl radical with  
10 alkylaromatics and benzylic alcohols.<sup>7,9</sup>

11  
12  
13  
14  
15  
16  
17  
18 The decrease of the PINO electron density can also be affected by replacement of the phenyl with  
19 an electron withdrawing *N*-heteroaromatic ring (*N*-hydroxyquinolinimide, NHQI, Figure 3). The  
20 corresponding *N*-oxyl radical (QINO) should be more reactive than PINO in HAT processes and  
21 therefore NHQI may serve as a better catalyst than NHPI in the oxidations of organic compounds  
22 using molecular oxygen as terminal oxidant. In this connection, Xia et al. showed that the catalytic  
23 activity of NHQI in the aerobic oxidation of toluene is significantly higher than that of NHPI either  
24 in the absence or in the presence of a metal cocatalysts.<sup>10</sup> More recently it was reported that NHQI,  
25 in combination with 4-carboxyl-*N*-hydroxyphthalimide, showed excellent activity in the aerobic  
26 oxidation of ethylbenzene.<sup>11</sup>



48 **Figure 3.** Structures of *N*-hydroxyphthalimide (NHPI), *N*-hydroxyquinolinimide (NHQI),  
49 phthalimide-*N*-oxyl radical (PINO) and quinolinimide *N*-oxyl radical (QINO)  
50  
51  
52

53  
54  
55 In this study we report the ultraviolet-visible (UV-vis) and electron paramagnetic resonance  
56 (EPR) spectroscopic characterization of QINO and a kinetic investigation of the HAT reactivity of  
57  
58  
59  
60

QINO with a series of organic substrates including aliphatic hydrocarbons, alkylaromatics, alcohols, ethers, aldehydes and amides. The results were compared with those found in the HAT processes promoted by PINO. Theoretical calculations using a density-functional theory (DFT) based technique was carried out for the HAT reactions of PINO and QINO with toluene, selected for the industrial relevance of the HAT from alkylaromatics to *N*-oxyl radicals,<sup>1</sup> in order to gain an insight into the energetics of the HAT process involving these species. Since an increase of the QINO reactivity in HAT process may result from the protonation or complexation with metal cations of the heteroaromatic nitrogen, kinetic studies have been also investigated in the presence of Brønsted and Lewis acids (HClO<sub>4</sub> and Mg(ClO<sub>4</sub>)<sub>2</sub>) employed at 0.15 M concentration.

## Results

### *Generation and characterization of QINO*

The QINO radical was generated in a quartz cuvette by adding a 0.5 M solution of cerium(IV) ammonium nitrate in acetonitrile to a 1.0 M solution of NHQI at 25 °C, after which the UV-vis spectrum was obtained. This method was used previously to characterize spectroscopically PINO and other transient *N*-oxyl radicals (Figure 4).<sup>3,12</sup>

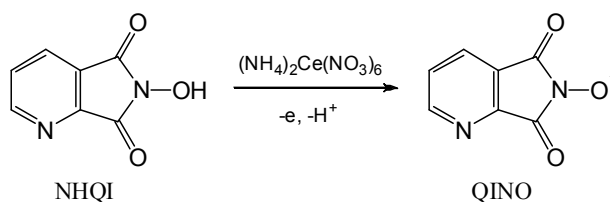
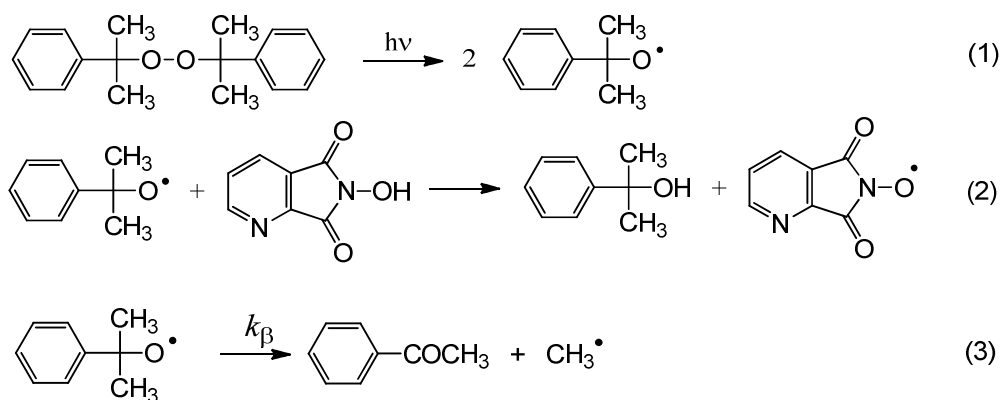


**Figure 4.** Generation of QINO by oxidation of NHQI with cerium(IV) ammonium nitrate

The UV-vis spectrum so-obtained has an absorption band centred at 380-390 nm. This band overlaps with the absorbance region of cerium salts (see Figure S1 in the SI). Better UV-vis spectroscopic characterization of QINO was obtained in a laser flash photolysis (LFP) experiment as described in Scheme 2.<sup>13,14</sup> Cumyloxyl radical (CumO<sup>•</sup>), generated by LFP at 355 nm of a 1 M

1  
2  
3 solution of dicumyl peroxide in N<sub>2</sub>-saturated acetonitrile at 25 °C, abstracts a hydrogen atom from  
4 NHQI (5 nM) yielding QINO (eq 2 in Scheme 2).<sup>15</sup> This hydrogen atom abstraction reaction occurs  
5  
6  
7 in competition with the β-scission of CumO• which leads to the formation of acetophenone and a  
8  
9 methyl radical (eq 3 in Scheme 2,  $k_{\beta} \sim 6.5 \times 10^5 \text{ s}^{-1}$  in CH<sub>3</sub>CN).<sup>13</sup> Figure 5 shows the time-resolved  
10  
11 spectra obtained. The first-order decay of the cumyloxyl radical recorded at its maximum  
12  
13 absorption wavelength (485 nm)<sup>14</sup> is accompanied by the build-up of the QINO absorption at 390  
14  
15  
16  
17 nm.



Scheme 2

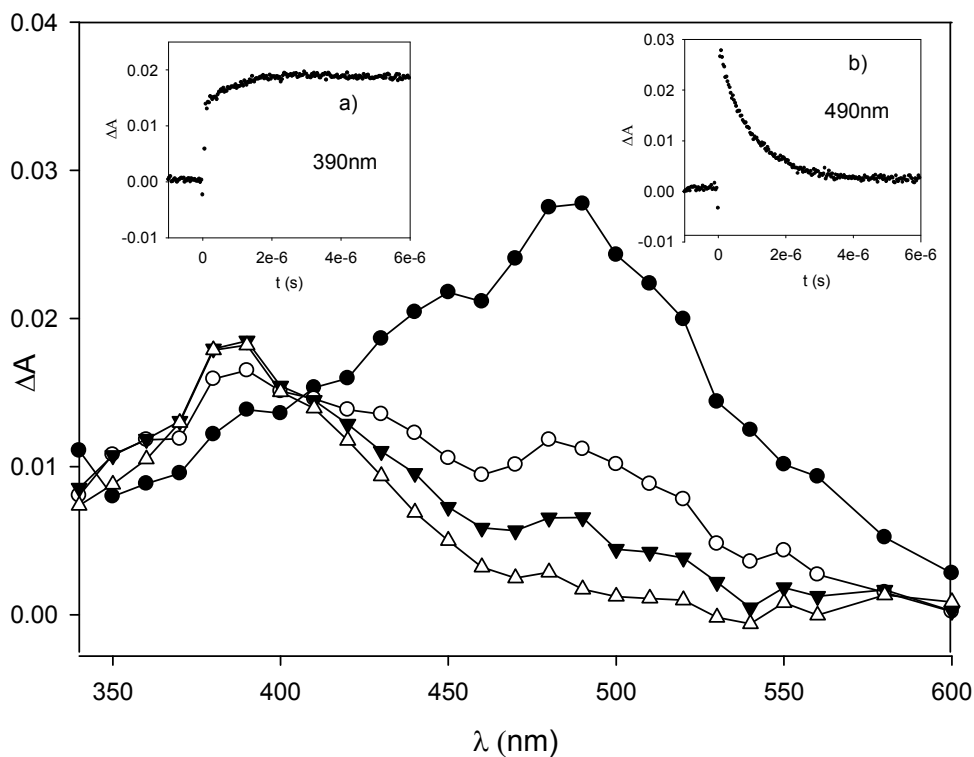


**Figure 5.** Transient absorption spectra measured 98 ns (●), 288 ns (○), 1 μs (▼) and 2 μs (Δ) after 355 nm laser excitation of a solution of dicumyl peroxide (1 M) and NHQI (5 mM) in CH<sub>3</sub>CN at 25 °C under N<sub>2</sub>. Inset a: first-order buildup of the QINO absorption at 390 nm. Inset b: first-order decay of the absorption of the cumyloxyl radical at 490 nm

The electron spin resonance spectrum of QINO was obtained at 298 K by UV photolysis of a CH<sub>3</sub>CN solution containing NHQI 10 mM and 10% (v/v) of di-*tert*-butyl peroxide. The spectrum (see Figure 6) shows three main lines due to the coupling of the unpaired electron with nitroxidic nitrogen ( $a_N = 4.57$  G).<sup>16</sup> Each lines shows also unresolved hyperfine structure due to small coupling of the unpaired electron with the nitrogen and hydrogen aromatic nuclei. A similar EPR spectrum of QINO was obtained by oxidation of NHQI with cerium(IV) ammonium nitrate (CAN) in CH<sub>3</sub>CN at 25 °C (see Figure S2 in the Supproting Information). The 2<sup>nd</sup> derivative spectrum clearly showed unresolved hyperfine structure due to small coupling of the unpaired electron with the nitrogen and hydrogen aromatic nuclei.



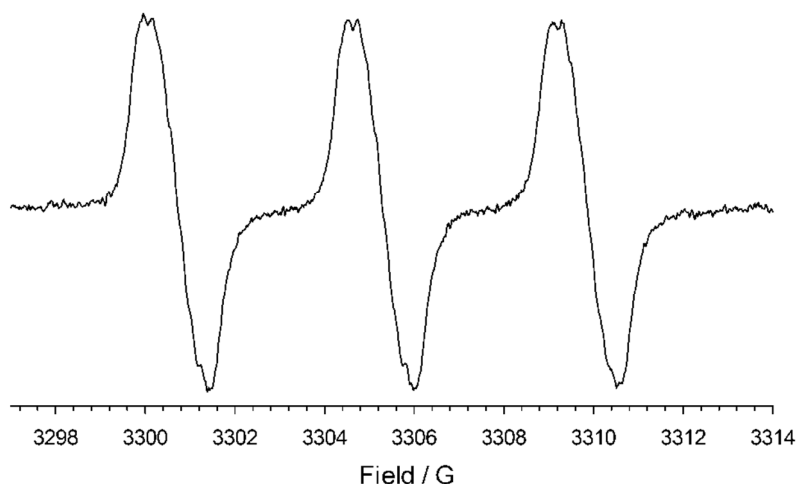
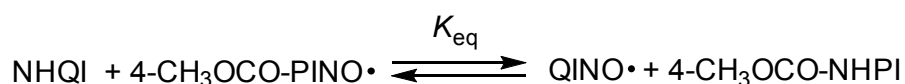


**Figure 6.** EPR spectrum of QINO recorded at 298 K during UV photolysis of a  $\text{CH}_3\text{CN}$  solution containing NQHI 10 mM and di-*tert*-butyl peroxide (10% v/v)

#### *NO-H Bond dissociation enthalpies (BDE) of NHQI*

The  $\text{BDE}_{\text{NO-H}}$  of NHQI is a parameter of fundamental importance for the analysis of the HAT reactivity of QINO. Its value, determined both experimentally and by theoretical calculations was compared with the  $\text{BDE}_{\text{NO-H}}$  value of NHPI previously determined with the same methodologies.<sup>2c,7a,d,8,17</sup> The experimental determination of O-H BDE was carried out by the EPR radical equilibration technique. For this purpose, we measured the equilibrium constant ( $K_{\text{eq}}$ ) for the hydrogen atom transfer reaction between NHQI and a NHPI derivative whose OH BDE was already known (Scheme 3). As a reference we choose 4- $\text{CH}_3\text{OCO-NHPI}$  which is characterized by an O-H BDE of 87.8 kcal/mol.<sup>18</sup>



**Scheme 3**

The initial concentration of *N*-hydroxyimides were used to calculate  $K_{\text{eq}}$ , while the relative radical concentration were determined by means of EPR spectroscopy (see details and Figure S3 in the

Supporting Information).<sup>19</sup> On the assumption that the entropic term can be neglected  $BDE_{\text{NHQI}} = BDE_{4\text{-CH}_3\text{OCO-NHPI}} - RT \ln(K_{\text{eq}})$ . From the experimentally determined radical concentrations, we obtained  $K_{\text{eq}} = 1.20$ , from which, an O-H BDE of  $87.7 \pm 0.6$  kcal/mol for NHQI was calculated.<sup>20</sup>

### Theoretical calculations

Density-functional theory (DFT) based calculations were performed to model the reactions of QINO and PINO radicals with toluene. The B3LYP/6-31+G(2d,2p)<sup>21</sup> level of theory was used as the underlying method. The effects of noncovalent interactions in the reacting systems were modeled with the dispersion-correcting potentials (DCPs) approach described previously.<sup>22</sup> Although there exists a number of more common approaches to correcting for the absence of dispersion in the B3LYP (and other) methods, we elected to use the DCP approach in order to obtain results comparable with those previously published for computational studies of the reactions between PINO and phenols. The method we applied is abbreviated as B3LYP-DCP/6-31+G(2d,2p).

We computed the energy-optimized structures of the reactants, pre- and post-reaction (noncovalently bound) complexes and the cisoid ( $\pi$ -stacked) and transoid (non-stacked) transition state (TS) structures in an implicit solvent field (acetonitrile) using the SMD model of Marenich et al.<sup>23</sup> All non-TS structures were verified to have only positive vibration frequencies and the TS structures had a single imaginary frequency that lead to the corresponding pre- and post-reaction species. The gas- and solvent-phase energy-optimized Cartesian coordinates of the reactants, pre- and post-reaction complexes, transition states and products are provided in the Supporting Information.

The O-H BDEs for NHQI and NHPI O-H BDEs were computed using the restricted open-shell (RO) version of CBS-QB3.<sup>24</sup> All calculations were performed using the Gaussian-09 program package.<sup>25</sup>

The (RO)CBS-QB3 method predicts the gas-phase O-H BDEs in NHQI and NHPI to be 84.0 and 83.1 kcal mol<sup>-1</sup> respectively,<sup>26</sup> with a difference of 0.9 kcal mol<sup>-1</sup> which is in line with the experimentally determined  $\Delta BDE_{\text{NO-H}}$  (0.7 kcal mol<sup>-1</sup>). The same approach predicts the C-H BDE

of the methyl group in toluene to be 89.7 kcal/mol. For comparison, the B3LYP-DCP/6-31+G(2d,2p) approach predicts the analogous BDEs in NHQI, NHPI, and toluene to be 80.0, 79.0, and 88.8 kcal/mol, respectively. We attribute the lack of agreement between the (RO)CBS-QB3 and B3LYP-DCP BDEs for NHQI and NHPI to delocalization errors associated with the underlying B3LYP functional. This suggests that the B3LYP-derived barrier heights and reaction endergonicity will be higher than the actual values (see below).

The calculated solvent phase free energies associated with the reaction of QINO and PINO with toluene in acetonitrile solvent are shown in Table 1. In the gas-phase, the reactants form fairly strongly bound pre-reaction complexes, with enthalpies of association of 8.4 (QINO) and 7.8 kcal/mol (PINO). However, the inclusion of entropic correction results in pre-reactions complex formation that are endergonic (2.6 kcal/mol in both cases, see Tables S1-S2 in the SI). The inclusion of estimates of the solvent effects increase the endergonicity of pre-reaction complex formation to 5.5 (QINO) and 4.6 (PINO) kcal/mol. These results are consistent with both the relatively high polarity of the radicals and the differential in the polarity between the radicals.

**Table 1.** Reaction free energies, relative to reactants, of the hydrogen atom transfer from toluene to QINO and PINO in acetonitrile solvent. The data were obtained using B3LYP-DCP/6-31+G(2d,2p) with the SMD solvation (acetonitrile) model. All values are in kcal/mol

Reaction step	QINO + Toluene	PINO + Toluene
Pre-reaction complex	5.5	4.6
Cisoid TS complex	19.6	20.6
Transoid TS complex	21.8	23
Post-reaction complex	13.3	14.4
Products	10.3	11.4

1  
2  
3 The TS structures associated with the HAT reaction of QINO and PINO with toluene were found to  
4 be  $\pi$ -stacked, or “cisoid” (Figure 7), rather than a “transoid” structure (i.e. non-stacked, or open, see  
5 Figure S43 in the SI). This finding is consistent with the calculated structure for the HAT identity  
6 reaction for the toluene/benzyl<sup>27</sup> and the phenol/phenoxy<sup>28</sup> couples. As was discussed in ref. 7, the  
7 overlap of the aromatic moieties results in some degree of noncovalent bonding interaction between  
8 them within the TS structure, thereby stabilizing the cisoid TS structure preferentially to the  
9 transoid structure. In the case of the QINO/PINO reactions with toluene, the cisoid transition state  
10 structures are 3.2 kcal/mol lower in free energy relative to transoid structures in the gas-phase (see  
11 Tables S1-S2 in the SI). The preferential stabilization of the cisoid TS structures persist in solvent  
12 but the differential between the cisoid and transoid structures is reduced by ca. 1 kcal/mol (see  
13 Tables S3-S4 in the SI), presumably because the transoid TS structures are more stabilized by  
14 interactions with the solvent field.

15  
16  
17  
18  
19  
20  
21  
22  
23  
24  
25  
26  
27  
28  
29 The calculated free energy barrier height for the reaction between QINO and toluene is 19.6  
30 kcal/mol. As expected on the basis of the arguments made above, this barrier is found to be 1  
31 kcal/mol lower than that associated with the PINO reaction. Both barriers are expected to be over-  
32 estimated by ca. 2-3 kcal/mol on the basis that B3LYP predicts a larger differential between the  
33 NHQI/NHPI O-H BDEs and the toluene methyl group C-H BDE than does (RO)CBS-QB3.

34  
35  
36  
37  
38  
39  
40  
41  
42  
43  
44  
45  
46  
47  
48  
49  
50  
51  
52  
53  
54  
55  
56  
57  
58  
59  
60  
The lower free energy barrier in the QINO-toluene HAT reaction is consistent with the fact that  
there is a higher degree of charge transfer between the reactants in this system as compared to that  
in the PINO-toluene reaction. For example, our solvent-phase calculations indicate that 0.47  
electrons are transferred from toluene to QINO-toluene in the cisoid TS complex, which is 0.06  
electrons higher than in the analogous PINO-toluene complex. For comparison, the degree of  
charge transfer system in the transoid TS structures is 2-4 fold lower. This supports the notion that  
the ring stacking interactions in the TS facilitates charge transfer and promotes HAT.

After the hydrogen atom transfer is completed, the calculations predict that the species involved in  
the reaction will not remain complexed in acetonitrile. The enthalpies/free energies associated with

1  
2  
3  
4  
5  
6  
7  
8  
9  
10  
11  
12  
13  
14  
15  
16  
17  
18  
19  
20  
21  
22  
23  
24  
25  
26  
27  
28  
29  
30  
31  
32  
33  
34  
35  
36  
37  
38  
39  
40  
41  
42  
43  
44  
45  
46  
47  
48  
49  
50  
51  
52  
53  
54  
55  
56  
57  
58  
59  
60

complexation within the post-reaction complex are predicted to be +3.4/+13.3 kcal/mol for NHQI-benzyl and +4.7/+14.4 kcal/mol for NHPI-benzyl, relative to the reactants in solvent. The final dissociated products of the HAT reaction in solvent are 10.3 (QINO) and 11.4 (PINO) kcal/mol higher in free energy than the reactants. On the basis of the differences between the B3LYP and (RO)CBS-QB3 bond dissociation energies, our expectation is that the free energies of the two reactions are closer to 7-8 kcal/mol.

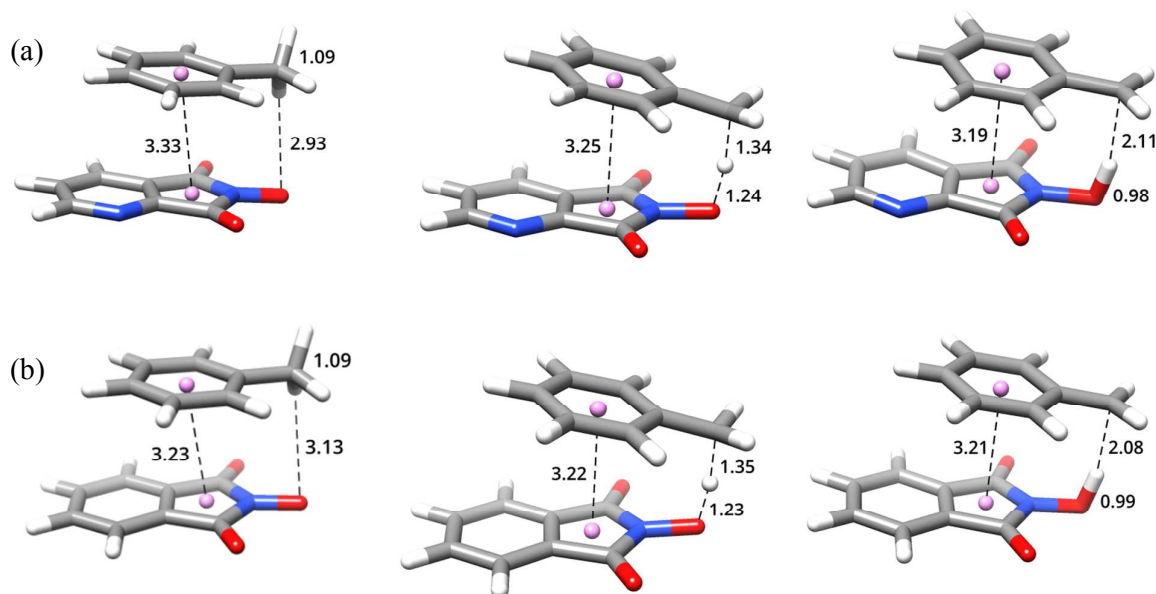
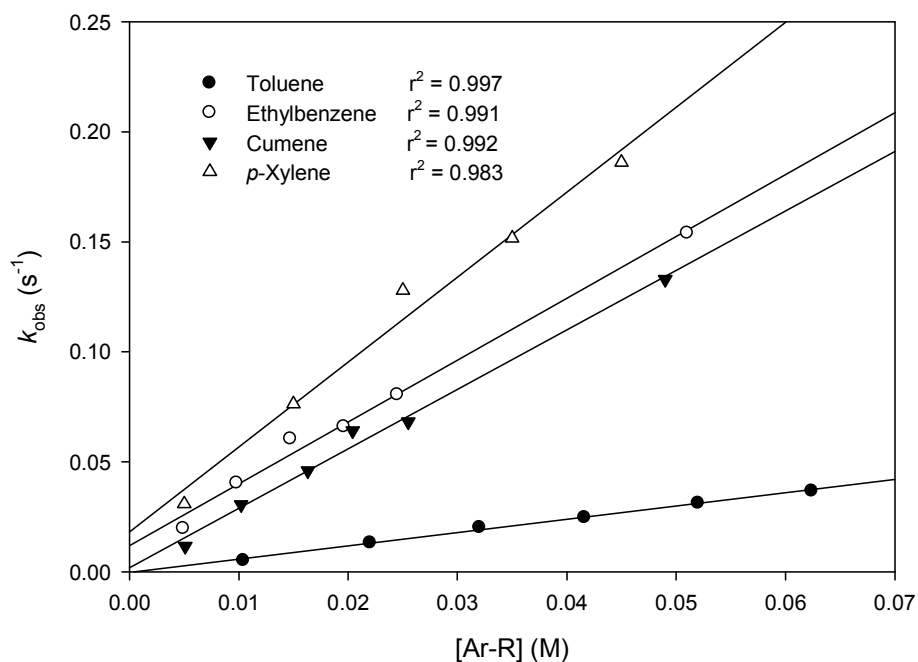


**Figure 7.** Optimized structures for the pre-reaction, transition state, and post-reaction structures for the reaction of (a) QINO and (b) PINO with toluene. Structures were obtained using the B3LYP-DCP/6-31+G(2d,2p) with the SMD solvation (acetonitrile) model. Key distances shown are in Angstroms. Key: Carbon = grey; Hydrogen = White; Oxygen = red; Nitrogen = blue. The geometric centers of the five- and six membered rings are shown as purple spheres.

#### *Kinetic study of the HAT from C-H bonds to QINO and PINO*

Kinetic studies were carried out by UV-vis spectrophotometry generating QINO and PINO by oxidation of NHQI and NHPI with cerium(IV) ammonium nitrate in CH<sub>3</sub>CN at T = 25 °C.<sup>3,12,29</sup> The decay of the *N*-oxyl radicals was recorded at 390 nm and 380 nm for QINO and PINO, respectively.

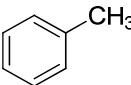
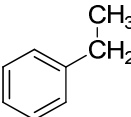
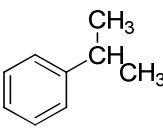
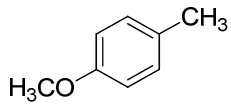
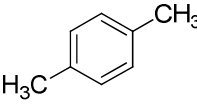
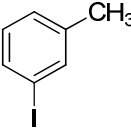
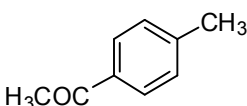
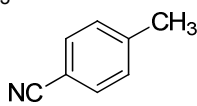
Using an excess of substrates (at least 10-fold) to attain pseudo first-order conditions, clean first order decays were observed with the H-abstraction rate faster than the spontaneous decay of the *N*-oxyl radicals and excellent linear fits were obtained by plotting the pseudo-first order rate constants ( $k_{\text{obs}}$ ) as a function of the concentration of hydrogen donors. From the slope of these plots, the second order rate constants for HAT ( $k_{\text{H}}$ ) were determined, as shown in Figure 8 for the reactions of QINO with alkylaromatics.<sup>30</sup>



**Figure 8.** Dependence of the observed rate constants ( $k_{\text{obs}}$ ) against [substrate] for the reactions of QINO with alkylaromatics measured in  $\text{CH}_3\text{CN}$  solution at  $T = 25^\circ\text{C}$  by following the decay of QINO at 390 nm.

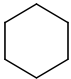
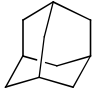
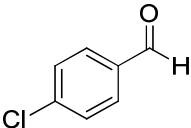
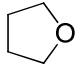
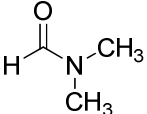
The  $k_{\text{H}}$  values are collected in Table 2 for the reactions of QINO and PINO with alkylaromatics and in Table 3 for the other hydrogen atom donors. In Table 2 are also reported the  $k_{\text{H}}$  values for the HAT reactions of QINO with alkylaromatics in the presence of either 0.15 M  $\text{HClO}_4$  or 0.15 M  $\text{Mg}(\text{ClO}_4)_2$  in  $\text{CH}_3\text{CN}$ . Linear plots of  $k_{\text{obs}}$  against [substrate] are reported in Figures S4-S39 in the Supporting Information.

**Table 2.** Second order rate constants ( $k_H$ ) for hydrogen atom transfer (HAT) from alkylaromatics to QINO and PINO measured in CH<sub>3</sub>CN at T = 25 °C.

Substrate	$k_H$ (M <sup>-1</sup> s <sup>-1</sup> ) <sup>a</sup>	
	QINO	PINO
	0.2 2.8 <sup>b</sup> 0.33 <sup>c</sup>	0.11
	1.5 28 <sup>b</sup> 2.4 <sup>c</sup>	0.95 <sup>d</sup> 1.17 <sup>d,e</sup>
	2.9 57 <sup>b</sup> 3.7 <sup>c</sup>	1.3
	1.3	0.93
	0.65 9.7 <sup>b</sup> 1.2 <sup>c</sup>	0.57 <sup>d</sup> 0.68 <sup>d,e</sup>
	0.15 1.9 <sup>b</sup>	0.11
	0.11 0.45 <sup>b</sup>	0.07
	0.036 0.11 <sup>b</sup>	0.022

<sup>a</sup> Average of at least three independent determinations. Error  $\pm$  5%. Statistically corrected for the number of labile hydrogens. Correlation coefficients  $0.982 < r^2 < 0.999$ . <sup>b</sup> In the presence of 0.15 M HClO<sub>4</sub>. <sup>c</sup> In the presence of 0.15 M Mg(ClO<sub>4</sub>)<sub>2</sub>. <sup>d</sup> See Ref. 12. <sup>e</sup> In the presence of 0.1 M HClO<sub>4</sub>.

**Table 3.** Second order rate constants ( $k_H$ ) for hydrogen atom transfer (HAT) from aliphatic hydrocarbons, alcohols, aldehydes, ethers and amides to QINO and PINO measured in CH<sub>3</sub>CN at T = 25 °C.

Substrate	$k_H$ ( $M^{-1}s^{-1}$ ) <sup>a</sup>	
	QINO	PINO
	0.034	0.014
	0.54	0.15
CH <sub>3</sub> OH	0.032	0.012
CH <sub>3</sub> CH <sub>2</sub> OH	0.55	0.29
(CH <sub>3</sub> ) <sub>2</sub> CHOH	3.8	2.1
	0.55	0.19
	2.2	1.0
	0.19	0.14 <sup>b</sup>

<sup>a</sup> Average of at least three independent determinations. Error  $\pm$  5%. Correlation coefficients  $0.972 < r^2 < 0.999$ . <sup>b</sup> See ref. 12.

### Discussion

The data shown in Tables 2-3 indicate that the presence of the *N*-heteroaromatic ring in QINO results in a significant increase in HAT rate constants involving all the substrates. The higher reactivity of QINO compared to PINO can be rationalized on the basis of both enthalpic and polar effects. We found that the  $BDE_{NO-H}$  value for NHQI determined experimentally by the EPR radical equilibration technique is ca 0.7 kcal/mol higher than that of NHPI, and 1.1 kcal/mol by the B3LYP-DCP approach in solvent. The introduction of an electron-withdrawing nitrogen atom into



1  
2  
3 the aromatic ring of NHQI results in a destabilization of the charge-separated resonance structure of  
4  
5 the *N*-oxyl radical (see Figure 2),<sup>2c</sup> thereby increasing the  $BDE_{NO-H}$ .  
6

7 The reactivity of *N*-oxyl radicals in the HAT processes is determined by both the enthalpic  
8  
9 requirements of the C-H and NO-H bond dissociation energies and by the polar effects that may  
10  
11 stabilize the activated complex.<sup>6</sup> The introduction of an N atom in the aromatic ring of QINO leads  
12  
13 to a stabilization of the activated complex by increasing the electron density on QINO. Figure 7  
14  
15 shows an example of these stabilizing effects in the TS for the HAT from substituted toluenes.  
16  
17

18 The computational modelling of the benzylic hydrogen abstraction from toluene by QINO and  
19  
20 PINO provides additional insights on the role of charge transfer stabilization of TS structures. The  
21  
22 hydrogen transfer occurs by the same mechanism described in the previous study on the reactions of  
23  
24 activated phenols with PINO and other *N*-oxyl radicals.<sup>6g,8</sup> The pre-reaction complex that is formed  
25  
26 between the reactants has a cisoid structure that is stabilized through  $\pi$ -stacking interactions (see  
27  
28 Figure 7). Relative to the separated reactants, the complexes have free energies of 5.5 (QINO) and  
29  
30 4.6 (PINO) kcal/mol. The cisoid arrangements are maintained in the TS structures, allowing a  
31  
32 charge transfer contribution to the HAT process through the  $\pi$ -overlap between the benzylic and  
33  
34 QINO aromatic rings.<sup>31</sup> The calculations support the expectation that the inclusion of a nitrogen  
35  
36 atom in the aryl ring of the abstracting radical, as in QINO, allows for a greater degree of charge  
37  
38 transfer in the TS. Specifically, 0.06 more electrons are transferred between the QINO and benzyl  
39  
40 moieties in the TS structure than in the analogous TS structure involving PINO.  
41  
42  
43  
44

45 The  $k_H$  values for the HAT from alkylaromatics to QINO reported in Table 2 show an increase  
46  
47 along the series cumene > ethylbenzene > toluene, as expected from the series of decreasing C-H  
48  
49 BDEs from the tertiary C-H bond of cumene ( $BDE = 83.2 \pm 1 \text{ kcal mol}^{-1}$ )<sup>32</sup> to the primary C-H  
50  
51 bond in toluene ( $BDE = 89.7 \pm 1.2 \text{ kcal mol}^{-1}$ )<sup>32</sup> and is in line with the HAT promoted by PINO in  
52  
53 acetic acid<sup>2b</sup> and in  $CH_3CN$  (see Table 2). For the series of substituted toluenes, as expected for a  
54  
55 HAT process promoted by electrophilic radicals and in accordance with the enthalpic and polar  
56  
57 effects discussed above, the  $k_H$  values increase with the electron donating strength of the aryl  
58  
59  
60

substituent. When the  $\log(k_X/k_H)$  values for the reactions of QINO with substituted toluenes were plotted against the Okamoto-Brown substituent constants  $\sigma^+$ , good Hammett-type correlations was obtained (Figure 9).<sup>33</sup> The negative  $\rho$  value (-0.99),<sup>34</sup> as well as the better linearity obtained with the  $\sigma^+$  rather than the  $\sigma$  constants, are in accordance with the significant polar effects associated to the development of a partial positive charge on the benzylic position in the HAT TS.

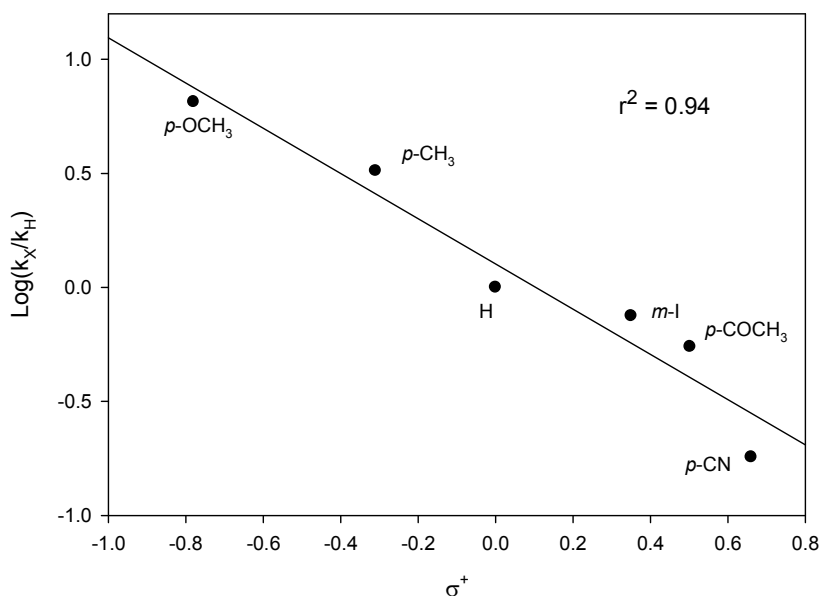


**Figure 9.** Hammett plot for the reaction of substituted toluenes with QINO in CH<sub>3</sub>CN at 25°C.

Table 3 shows the rate constants for the HAT from a series of hydrogen atom donors. Rate constants for the HAT from C-H bonds in unactivated aliphatic hydrocarbons (cyclohexane and adamantane), as expected, are significantly lower than those determined with alkylaromatics. The increase in reactivity observed for QINO as compared to PINO is of fundamental importance with these substrates which are characterized by relatively high C-H BDE values (99.5 kcal/mol for cyclohexane, 96.2 and 98.4 kcal/mol for tertiary and secondary C-H bonds respectively in adamantane).<sup>32</sup>

The higher reactivity observed in HAT from alcohols, ethers (THF), amides (DMF) is in line with the enthalpic and polar effects associated with electron rich C-H bonds in  $\alpha$  position to heteroatoms,

able to stabilize the partial positive charge that develops on carbon in the HAT.

The presence of the heteroaromatic nitrogen in NHQI allows a further activation of the corresponding *N*-oxyl radical in HAT processes by adding Brønsted or Lewis acids in fact the protonation or coordination of the N atom decreases the electron density on QINO (Figure 10).<sup>35</sup>

An increased electrophilicity of QINO would result as a consequence of the destabilization of the charge separated resonance structures shown in Figure 10. In this context, it should be mentioned that through complexation of NHQI with cobalt and copper ions it was possible to improve the activity of NHQI in the oxidation of toluene. This activating effect has been interpreted on the basis of an electron-withdrawing effect produced by the complexation of the *N*-heteroaromatic ring with the metal salts. The complexation of NHQI with CuCl<sub>2</sub> has been also confirmed through real time *in situ* FTIR spectral analysis.<sup>10</sup>

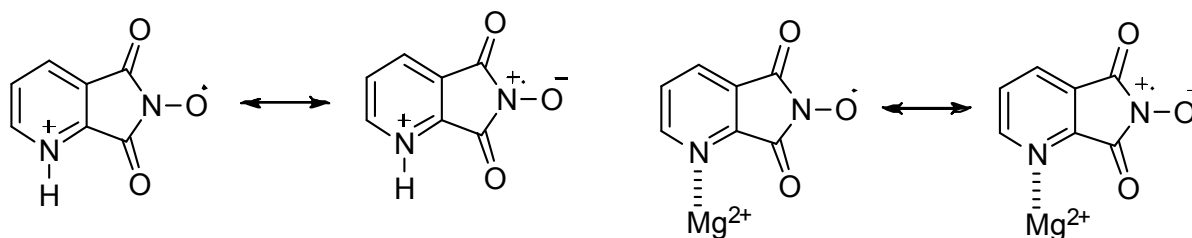


**Figure 10.** Resonance structures of QINO in the presence of Brønsted or Lewis acids

In order to investigate the effect of acid additives on the QINO reactivity in HAT process, kinetic studies with alkylaromatics were also investigated in the presence of 0.15 M HClO<sub>4</sub> and 0.15 M Mg(ClO<sub>4</sub>)<sub>2</sub>.

Considering the electron withdrawing effect of the two imidic carbonyls, the p*K*<sub>a</sub> value for piridinium cation (p*K*<sub>a</sub> = 12.3 in CH<sub>3</sub>CN)<sup>36</sup> is much higher than that of HClO<sub>4</sub> (p*K*<sub>a</sub> = 2.0 in CH<sub>3</sub>CN),<sup>36</sup> thus the protonation of QINO to give QINOH<sup>+</sup>• in 0.15 M HClO<sub>4</sub> should be almost quantitative. Accordingly, a variation of the UV-vis spectra of QINO, generated by oxidation of NHQI (1.0 mM) with CAN (0.5 mM) in CH<sub>3</sub>CN, was observed as a function of increasing the

[HClO<sub>4</sub>] up to the value of 0.15 M (see Figure S40 in the SI).

The data reported in Table 2 indicate increases in reactivity of more than one order of magnitude, in the presence of 0.15 M HClO<sub>4</sub> for all the alkylaromatics tested. This is consistent with the previsions based on the favorable enthalpic and polar effects associated with the protonation of QINO. It should be noted that a smaller increase of the  $k_H$  value for the HAT from alkylaromatics (ethylbenzene and *p*-xylene, see Table 2) in the presence of HClO<sub>4</sub> was also observed for PINO in a previous study.<sup>12</sup> The increase of reactivity with PINO has been attributed to the protonation of imidic carbonyl groups.

Compared to HClO<sub>4</sub> a lower degree of activation was observed in the presence of 0.15 M MgClO<sub>4</sub>. For example the  $k_H$  value for the HAT from toluene to QINO increased from 0.2 M<sup>-1</sup>s<sup>-1</sup> to 0.33 M<sup>-1</sup>s<sup>-1</sup> by addition of the Lewis acid. This behavior reflects a minor decrease of electron density in QINO as compared to the perchloric acid.

The increase of QINO electrophilicity caused by the protonation of the heteroaromatic nitrogen is in accordance with the more negative  $\rho$  value (-1.8) determined in the Hammett correlation (see Figure S42 in the SI) for the HAT process from substituted toluenes to QINO observed in the presence of 0.15 M HClO<sub>4</sub>.

In conclusion the results reported in this study clearly indicate that QINO has greater hydrogen abstracting ability than PINO in HAT processes from all the classes of organic compounds investigated. This supports the use of *N*-hydroxyquinolinimide (NHQI) as a convenient substituted for *N*-hydroxyphthalimide (NHPI) in the catalytic aerobic oxidations of substrates such as aliphatic hydrocarbons that have relatively high C-H bond dissociation energies.

## Experimental Section

### Materials

1  
2  
3 Acetonitrile (HPLC grade), *N*-hydroxyphthalimide (NHPI), (NH<sub>4</sub>)<sub>2</sub>Ce(NO<sub>3</sub>)<sub>6</sub>, Mg(ClO<sub>4</sub>)<sub>2</sub> and  
4 HClO<sub>4</sub> were commercially available and used as received. *N*-hydroxyquinolinimide (NHQI) was  
5 synthesized by reaction of pyridine-2,3-dicarboxylic acid anhydride<sup>37</sup> with hydroxylamine  
6 hydrochloride following a procedure reported in the literature.<sup>10</sup>  
7  
8

9  
10  
11 Toluene, ethylbenzene, cumene, *p*-xylene, *p*-methoxytoluene, *m*-iodotoluene, 4-  
12 methylacetophenone, *p*-tolunitrile, cyclohexane, adamantane, methanol, ethanol, 2-propanol,  
13 tetrahydrofuran, *N,N*-dimethylformamide, *p*-chlorobenzaldehyde were commercially available at  
14 their highest purity and used as received.  
15  
16  
17  
18  
19

### 20 Kinetic Studies

21  
22 QINO and PINO were generated by oxidation of the corresponding *N*-hydroxyimides (NHQI and  
23 NHPI) (1 mM) with cerium(IV) ammonium nitrate (CAN) 0.4 mM in CH<sub>3</sub>CN at 25 °C.  
24

25  
26 HAT reactions of QINO with alkylaromatics were investigated either in the absence of acid  
27 additives or in the presence of HClO<sub>4</sub> (0.15 M) or Mg(ClO<sub>4</sub>)<sub>2</sub> (0.15 M). After the generation of the  
28 *N*-oxyl radicals, an excess of substrate was added in order to operate under pseudo first-order  
29 conditions (final concentration 1.8-300 mM) and the absorbance change was monitored at 390 nm  
30 for QINO and 380 nm for PINO. For all the substrates investigated each kinetic trace obeyed a first-  
31 order kinetics. Second-order rate constants were obtained from the slopes of plots of the observed  
32 rate constants  $k_{\text{obs}}$  vs substrate concentration. Rate constants are reported as the average of at least  
33 three independent determinations with an error  $\pm$  5%.  
34  
35  
36  
37  
38  
39  
40  
41  
42  
43  
44  
45  
46

47 **Acknowledgements.** Thanks are due to the Ministero dell'Istruzione, dell'Università e della Ricerca  
48 (MIUR) for financial support and to the CIRCC, Interuniversity Consortium of Chemical Catalysis  
49 and Reactivity. We thank Prof. M. Bietti and Dr. M. Salamone for the use of LFP equipment. GAD  
50 thanks the National Sciences and Engineering Research Council of Canada, the Canadian  
51 Foundation for Innovation and the University of British Columbia for financial support and  
52 Compute Canada for access to computational resources.  
53  
54  
55  
56  
57  
58  
59  
60

1  
2  
3  
4  
5 **Supporting Information Available:** Instrumentation. Determination of the O-H BDE values by  
6  
7 EPR measurements. UV-vis spectroscopic characterization of QINO. EPR spectrum of QINO  
8  
9 obtained by oxidation of NHQI with cerium(IV) ammonium nitrate (CAN) in CH<sub>3</sub>CN at 25 °C.  
10  
11 EPR spectrum of irradiated CH<sub>3</sub>CN solution containing di-*tert*-butyl peroxide, NHQI and 4-  
12  
13 CH<sub>3</sub>OCO-NHPI. Plots of  $k_{\text{obs}}$  vs [substrate] for the reactions of QINO and PINO with  
14  
15 alkylaromatics, aliphatic hydrocarbons, alcohols, aldehydes, ethers and amides. UV-vis spectra of  
16  
17 QINO in MeCN/[HClO<sub>4</sub>] (0-0.2 M). Hammett plot for the HAT process from substituted toluenes to  
18  
19 PINO in CH<sub>3</sub>CN and to QINO in CH<sub>3</sub>CN/HClO<sub>4</sub> 0.15 M. Gas- and solvent-phase (acetonitrile)  
20  
21 computational results for HAT reaction of QINO/PINO with toluene. Optimized structures of the  
22  
23 transition states for the reaction of QINO and PINO with toluene. Cartesian coordinates of the  
24  
25 optimized structures of the reaction steps. This material is available free of charge via the Internet at  
26  
27 <http://pubs.acs.org>.  
28  
29  
30  
31  
32  
33

### 34 **References and notes**

- 35  
36 (1) (a) Ishii, Y.; Sakaguchi, S.; Iwahama, T. *Adv. Synth. Catal.* **2001**, *343*, 393-427. (b) Sheldon,  
37  
38 R. A.; Arends, I. W. C. E. *Adv. Synth. Catal.* **2004**, *346*, 1051-1071. (c) Recupero, F.; Punta, C.  
39  
40 *Chem. Rev.*, **2007**, *107*, 3800-3842. (d) Coseri, S. *Catal. Rev.* **2009**, *51*, 218-292. (e) Melone, L.;  
41  
42 Punta, C. *Beilstein J. Org. Chem.* **2013**, *9*, 1296-1310. (f) Wertz, S.; Studer, A. *Green Chem.* **2013**,  
43  
44 *15*, 3116-3134. (g) Chen, K.; Zhang, P.; Wang, Y.; Li, H. *Green Chem.* **2014**, *16*, 2344-2374, and  
45  
46 references cited therein.  
47  
48  
49  
50 (2) (a) Ueda, C.; Noyama, M.; Ohmori, H.; Masui, M. *Chem Pharm. Bull.* **1987**, *35*, 1372-1377.  
51  
52 (b) Koshino, N.; Cai, Y.; Espenson, J. H. *J. Phys. Chem. A* **2003**, *107*, 4262-4267. (c) Amorati, R.;  
53  
54 Lucarini, M.; Mugnaini, V.; Pedulli, G. F.; Minisci, F.; Recupero, F.; Fontana, F.; Astolfi, P.; Greci,  
55  
56  
57  
58  
59  
60

1  
2  
3 L. *J. Org. Chem.* **2003**, *68*, 1747–1754. (d) Koshino, N.; Saha, B.; Espenson, J. H. *J. Org. Chem*  
4  
5 **2003**, *68*, 9364-9370.

6  
7  
8 (3) (a) Galli, C.; Gentili, P.; Lanzalunga, O.; Lucarini, M.; Pedulli, G. F. *Chem. Commun.*, **2004**,  
9  
10 2356-2357. (b) Brandi, P.; Galli, C.; Gentili, P. *J. Org. Chem.*, **2005**, *70*, 9521-9528. (c) Galli, C.;  
11  
12 Gentili, P.; Lanzalunga, O. *Angew. Chem. Int. Ed.* **2008**, *47*, 4790-4796. (d) Coniglio, A.; Galli, C.;  
13  
14 Gentili, P.; Vadalà, R. *J. Mol. Catal. B: Enzym.*, **2008**, *50*, 40-49. (e) Coniglio, A.; Galli, C.;  
15  
16 Gentili, P.; Vadalà, R. *Org. Biomol. Chem.*, **2009**, *7*, 155-160.

17  
18  
19  
20 (4) The initial value of 88.1 kcal mol<sup>-1</sup> has been recalculated using the corrected O-H BDE  
21  
22 value for the reference compound BHT (ref. 5).

23  
24  
25 (5) (a) Mulder, P.; Korth, H.-G.; Pratt, D. A.; DiLabio, G. A.; Valgimigli, L.; Pedulli, G. F.;  
26  
27 Ingold, K. U. *J. Phys. Chem. A* **2005**, *109*, 2647-2655. (b) Capraro, M. G.; Franchi, P.; Lanzalunga,  
28  
29 O.; Lapi, A.; Lucarini, M. *J. Org. Chem.* **2014**, *79*, 6435-6443.

30  
31  
32  
33 (6) (a) Minisci, F.; Punta, C.; Recupero, F.; Fontana, F.; Pedulli, G. F. *J. Org. Chem.* **2002**, *67*,  
34  
35 2671-2676. (b) Minisci, F.; Punta, C.; Recupero, F.; Fontana, F.; Pedulli, G. F. *Chem. Commun.*  
36  
37 **2002**, 688-689. (c) Cecchetto, A.; Minisci, F.; Recupero, F.; Fontana, F.; Pedulli, G. F. *Tetrahedron*  
38  
39 *Lett.* **2002**, *43*, 3605-3607. (d) Minisci, F.; Recupero, F.; Cecchetto, A.; Gambarotti, C.; Punta, C.;  
40  
41 Faletti, R.; Paganelli, R.; Pedulli, G. F. *Eur. J. Org. Chem.* **2004**, 109-119. (e) Baciocchi, E.; Gerini,  
42  
43 M. F.; Lanzalunga O. *J. Org. Chem.* **2004**, *69*, 8963-8966. (f) Minisci, F.; Punta, C.; Recupero, F. *J.*  
44  
45 *Mol. Catal. A: Chem.* **2006**, *251*, 129-149. (g) D'Alfonso, C.; Bietti, M.; DiLabio, G. A.;  
46  
47 Lanzalunga, O.; Salamone, M. *J. Org. Chem.* **2013**, *78*, 1026-1037.

48  
49  
50  
51 (7) (a) Annunziatini, C.; Gerini, M. F.; Lanzalunga O.; Lucarini, M. *J. Org. Chem.* **2004**, *69*, 3431-  
52  
53 3438. (b) Cai, Y.; Koshino, N.; Saha, B.; Espenson, J. H. *J. Org. Chem* **2005**, *70*, 238-243. (c)  
54  
55 Annunziatini, C.; Baiocco, P.; Gerini, M. F.; Lanzalunga O.; Sjogren, B. *J. Mol. Catal. B: Enzym.*  
56  
57 **2005**, *32*, 89-96. (d) Sun, Y.; Zhang, W.; Hu, X.; Li, H. *J. Phys. Chem. B* **2010**, *114*, 4862-4869. (e)  
58  
59  
60

1  
2  
3 D'Alfonso, C.; Lanzalunga, A.; Lapi, A.; Vadalà, R. *Tetrahedron*, **2014**, *70*, 3049-3055. (f) Chen,  
4 K.; Yao, J.; Chen, Z.; Li, H. *J. Catal.* **2015**, *331*, 76-85.

7  
8 (8) Mazzonna, M.; Bietti, M.; DiLabio, G. A.; Lanzalunga, O.; Salamone, M. *J. Org. Chem.* **2014**,  
9 *79*, 5209-5218.

12  
13 (9) (a) Wentzel, B. B.; Donners, M. P. J.; Alsters, P. L.; Feiters, M. C.; Nolte, R. J. M. *Tetrahedron*,  
14 **2000**, *56*, 7797-7803. (b) Zhang, Q.; Chen, H.; Ma, H.; Miao, H.; Zhang, Z.; Sun, Z.; Xu, J. *J.*  
15 *Chem. Technol. Biotechnol.* **2008**, *83*, 1364-1369.

18  
19 (10) Zhang, Q.; Chen, C.; Xu, J.; Wang, F.; Gao, J.; Xia, C. *Adv. Synth. Catal.* **2011**, *353*, 226-230.

22  
23 (11) Zhao, Q.; Chen, K.; Zhang, W.; Yao, Y.; Li, H. *J. Mol. Catal. A: Chem.* **2015**, *402*, 79-82.

26  
27 (12) Bietti, M.; Forcina, V.; Lanzalunga, O.; Lapi, A.; Martin, T.; Mazzonna, M.; Salamone, M. *J.*  
28 *Org. Chem.* **2016**, *81*, 11924-11931.

31  
32 (13) Avila, D. V.; Brown, C. E.; Ingold, K. U.; Luszytk, J. *J. Am. Chem. Soc.* **1993**, *115*, 466-470.

35  
36 (14) (a) Avila, D. V.; Luszytk, J.; Ingold, K. U. *J. Am. Chem. Soc.* **1992**, *114*, 6576-6577. (b) Avila,  
37 D. V.; Ingold, K. U.; Di Nardo, A. A.; Zerbetto, F.; Zgierki, M. Z.; Luszytk, J. *J. Am. Chem. Soc.*  
38 **1995**, *117*, 2711-2718.

41  
42 (15) (a) Coseri, S.; Mendenhall, G. D.; Ingold, K. U. *J. Org. Chem.* **2005**, *70*, 4629-4636. (b)  
43 Baciocchi, E.; Bietti, M.; Gerini, M. F.; Lanzalunga O. *J. Org. Chem.* **2005**, *70*, 5144-5149. (c)  
44 Baciocchi, E.; Bietti, M.; Di Fusco, M.; Lanzalunga, *J. Org. Chem.* **2007**, *72*, 8748-8754.

47  
48 (16) The  $a_N$  value of QINO is higher than that previously reported for PINO ( $a_N = 4.76$ ) in  
49 accordance with the electron withdrawing effect of the QINO *N*-heteroaromatic ring (see ref. 7a).

52  
53 (17) Da Silva, G.; Bozzelli, J. W. *J. Phys. Chem. C* **2007**, *111*, 5760-5765.



1  
2  
3 (18) The value of 88.9 kcal mol<sup>-1</sup> reported in ref. 7a has been recalculated using the corrected O-H  
4 BDE value for the reference compound BHT (ref. 5).  
5  
6

7  
8 (19) Franchi, P.; Mezzina, E.; Lucarini, M. *J. Am. Chem. Soc.* **2014**, *136*, 1250–1252.  
9

10  
11 (20) The error in the BDE measured by EPR ( $\pm 0.6$  kcal/mol) is related to the error reported for the  
12 original BDE measurement of NHPI used as reference (ref. 2c). However,  $\Delta$ BDEs errors in the EPR  
13 measurements are generally smaller (less than 0.3 kcal/mol). The accuracy of the EPR method relies  
14 on the fact that even relatively large errors in the measurement of radical concentrations and  
15 therefore of the equilibrium constant,  $K_{eq}$ , give rise to small errors in the  $\Delta$ BDEs because of the  
16 logarithmic relation connecting these two quantities.  
17  
18  
19  
20  
21  
22  
23

24  
25 (21) (a) Becke, A. D. *J. Chem. Phys.* **1993**, *98*, 5648–5652. (b) Lee, C.; Yang, W.; Parr, R. G. *Phys.*  
26 *Rev. B* **1988**, *37*, 785–789.  
27

28  
29  
30 (22) (a) Torres, E; DiLabio, G. A. *J. Phys. Chem. Lett.* **2012**, *3*, 1738-1744. (b) DiLabio, G. A.;  
31 Koleini, M.; Torres, E. *Theor. Chem. Acc.* **2013**, *132*, 1389.  
32  
33

34  
35 (23) Marenich, A. V.; Cramer, C. J.; Truhlar, D. G. *J. Phys. Chem. B* **2009**, *113*, 6378-6396.  
36  
37

38  
39 (24) Montgomery, J. A., Jr.; Frisch, M. J.; Ochterski, J. W.; Petersson, G. A. *J. Chem. Phys.* **2000**,  
40 *112*, 6532–6542.  
41  
42

43  
44 (25) Frisch, M. J.; Trucks, G. W.; Schlegel, H. B.; Scuseria, G. E.; Robb, M. A.; Cheeseman, J. R.;  
45 Scalmani, G.; Barone, V.; Mennucci, B.; Petersson, G. A. et al. Gaussian 09, revision D.01;  
46 Gaussian, Inc.: Wallingford, CT, 2009.  
47  
48

49  
50 (26) The computed gas-phase BDEs are lower than the experimental BDE values measured in polar  
51 solvents due to hydrogen bond of the *N*-hydroxylamines with the solvent, see ref. 8.  
52  
53  
54

55  
56 (27) DiLabio, G. A.; Johnson, E. R. *J. Am. Chem. Soc.* **2007**, *129*, 6199-6203.  
57  
58  
59  
60

1  
2  
3 (28) Harshan, A. K.; Soudackov, A. V.; Hammes-Sciffer, S. *J. Am. Chem. Soc.* **2015**, *137*, 13545-  
4  
5 13555.

6  
7  
8 (29) The use of LFP technique for the generation and reactivity studies of short-lived aminoxyl  
9  
10 radicals is limited to very fast reaction processes (in the  $\mu\text{s}$  and ms timescale, see refs. 8, 13b-c),  
11  
12 much faster than those reported in the present study.

13  
14  
15 (30) The pseudo first-order rate constant for the decay of QINO is described by the equation  $k_{\text{obs}} =$   
16  
17  $k_{\text{d}} + k_{\text{H}} [\text{Ar-R}]$  where  $k_{\text{d}}$  is the QINO self decay rate constant. Thus in the plot of  $k_{\text{obs}}$  vs  $[\text{Ar-R}]$  the  
18  
19 intercept on the  $k_{\text{obs}}$  axis ( $[\text{Ar-R}] = 0$ ) should not be on the origin but should be equal to  $k_{\text{d}}$ . Since  
20  
21 the extrapolated intercept value is always subjected to significant errors, a precise  $k_{\text{d}}$  determination  
22  
23 using this approach is not allowed.

24  
25  
26  
27 (31) It is rather difficult to determine with accuracy the contribution of charge transfer from  $\pi$ -  
28  
29 stacking between the aryl rings of PINO/QINO and aromatic substrates to the HAT process since it  
30  
31 is summed to the enthalpic and other polar effects, also present in the non-aryl hydrocarbons. On  
32  
33 these basis a direct comparison of the relative weight of these effects with different substrates is not  
34  
35 possible.

36  
37  
38  
39 (32) Luo, Y.-R. *Comprehensive Handbook of Chemical Bond Energies*, CRC Press: Boca Raton,  
40  
41 2007.

42  
43  
44 (33) A similar behaviour in Hammett type correlations has been reported for hydrogen abstraction  
45  
46 promoted by other electrophilic radicals. Pryor, W. A.; Lin, T. H.; Stanley, J. P.; Henderson, R. W.  
47  
48 *J. Am. Chem. Soc.* **1973**, *95*, 6993. Walling, C.; Jacknow, B. B. *J. Am. Chem. Soc.* **1960**, *82*, 6113.  
49  
50 Gilliom, R. D.; Ward, B. F., Jr. *J. Am. Chem. Soc.* **1965**, *87*, 3944. Kennedy, B. R.; Ingold, K. U.  
51  
52 *Can. J. Chem.* **1966**, *44*, 2381. Russell, G. A.; Williamson, R. C., Jr. *J. Am. Chem. Soc.* **1964**, *86*,  
53  
54 2357. Pearson, R. E.; Martin, J. C. *J. Am. Chem. Soc.* **1963**, *85*, 354. Huyser, E. S. *J. Am. Chem.*  
55  
56 *Soc.* **1960**, *82*, 394.

1  
2  
3 (34) The  $\rho$  value is in line with those determined for the reactions of substituted toluenes with PINO  
4  
5 in AcOH (-1.3) (ref. 2d) and in CH<sub>3</sub>CN (-1.0, see Figure S41 in the Supporting Information)  
6  
7

8 (35) The good hydrogen abstracting ability of QINOH<sup>+</sup>, generated from acid-base reaction of  
9  
10 NHQI and 4-carboxyl-*N*-hydroxyphthalimide, was taken into account to explain the high catalytic  
11  
12 activity in the aerobic oxidation of ethylbenzene (ref. 11).  
13  
14

15 (36) Izutsu, K. *Acid-base Dissociation Constant in Dipolar Aprotic Solvents*, Alden Press Oxford  
16  
17 (1990).  
18  
19

20 (37) Gould, K. J.; Hacker, N. P.; McOmie, J. F. W.; Perry, D. H. *J. Chem. Soc. Perkin Trans. 1*  
21  
22 **1980**, 1834-1840.  
23  
24  
25  
26  
27  
28  
29  
30  
31  
32  
33  
34  
35  
36  
37  
38  
39  
40  
41  
42  
43  
44  
45  
46  
47  
48  
49  
50  
51  
52  
53  
54  
55  
56  
57  
58  
59  
60

## Table of Contents Graphic

